Construction and Building Materials 301 (2021) 124113

Contents lists available at ScienceDirect

Construction and Building Materials

journal homepage: www.elsevier.com/locate/conbuildmat

Effect of basalt fiber on metakaolin-based geopolymer mortars containing rilem, basalt and recycled waste concrete aggregates

Furkan Şahin [a], Mucteba Uysal [b,*], Orhan Canpolat [b], Yurdakul Aygörmez [b], Turgay Cosgun [a], Heydar Dehghanpour [c]

[a] Istanbul University-Cerrahpasa, Civil Engineering Department, Avcilar Campus, Istanbul, Turkey
[b] Yildiz Technical University, Civil Engineering Department, Davutpasa Campus, Istanbul, Turkey
[c] Sakarya University, Civil Engineering Department, Sakarya, Turkey

ARTICLE INFO

Keywords:
Geopolymer
Metakaolin
Basalt fiber
Recycled waste concrete
Basalt sand
High-temperature
Freeze-thaw

ABSTRACT

With the development of technology, it is important to recommend new environmentally friendly materials instead of cement, which is the main binder of concrete. Recently, geopolymer mortars have been the focus of many researchers to achieve this goal. In this study, the effects of three different basalt fiber (BF) ratios on the metakaolin (MK)-based geopolymer mortars produced with three different aggregate types were investigated. By adding 0.0, 0.4, 0.8, and 1.2% BF for each group aggregate, a total of 12 different geopolymer mixtures were obtained. In the mixtures, metakaolin activated with sodium hydroxide (NaOH) and sodium silicate (Na_2SiO_3) was used as the main binder. Rilem sand (RS), basalt Sand (BS), and recycled waste concrete (RWC) were used separately as filling materials. Mechanical strengths of 7, 28, and 56-day specimens obtained from all mixtures were tested. Ultrasonic pulse velocity (UPV), high-temperature, abrasion, freeze–thaw, and porosity tests were performed for the mortars produced. According to the results, positive effects were observed on all properties due to the more systematic performance of geopolymer samples with the addition of basalt fiber. According to the results, basalt fiber had positive effects, especially when 0.8–1.2% was used. When the results were examined, it was able to create an increase of up to 25% in the compressive strength results and 50% in the flexural strength results. Also, although the properties of geopolymers produced with recycled aggregate were inferior to the others, the results obtained were quite acceptable values for the application. With the basalt sand effect, higher results were obtained by obtaining a harder and more dense structure than others.

1. Introduction

Geopolymer composites, which are agreed as an alternative to Portland cement, were first named by Davidovits in 1978 [1]. The main material of these three-dimensional amorphous products is aluminosilicates. Different pozzolanic materials are used to increase the strength and durability performance of geopolymer mortars. Metakaolin is a type of pozzolanic material obtained by calcining kaolin [2]. In other words, MK is a pozzolana material produced by heating kaolin-containing clays in a temperature range of about 600–900 °C [3]. This pozzolanic material, used as a binder in geopolymer mortars, is a dehydroxylated form of the clay mineral kaolinite associated with the $Al_2Si_2O_5(OH)_4 \rightarrow Al_2O_3{\bullet}2SiO_2 + 2H_2O$ reaction [4]. The chemical formula of metakaolin is $Al_2O_3{\bullet}2SiO_2$ [5]. This pozzolanic material consists of 50–55% SiO_2 and 40–45% Al_2O_3 [4]. Alkali-activation is required for metakaolin-based materials to be used in geopolymer mortars. In studies conducted by different authors, sodium hydroxide (NaOH) and sodium silicate (Na_2SiO_3) were used for alkali activation of metakaolin [6]. To reduce the environmental effect of the cement industries, it is recommended to use MK instead of cement in new generation concretes [4]. MK improves the physical and mechanical properties of mortar as well as being environmentally friendly [7–8].

High results have been obtained in studies where Rilem sand was used in geopolymer mortars [7–8]. However, the cost of Rilem sand and limited resources have given importance to the search for alternative sand. Recycled concrete is derived from collapsed or demolished structures (building, bridge, and pavement, etc.) [9]. To reduce the natural aggregates consumption by this method and to take advantage of non-renewable materials, waste concrete has been evaluated as a source material [10–12]. Mechanical properties, workability, and durability

* Corresponding author.
E-mail addresses: mucteba@yildiz.edu.tr (M. Uysal), canpolat@yildiz.edu.tr (O. Canpolat), aygormez@yildiz.edu.tr (Y. Aygörmez), costur@iuc.edu.tr (T. Cosgun).

https://doi.org/10.1016/j.conbuildmat.2021.124113
Received 22 March 2021; Received in revised form 19 May 2021; Accepted 26 June 2021
Available online 5 July 2021
0950-0618/© 2021 Elsevier Ltd. All rights reserved.

properties were investigated in studies related to the use of waste concrete as aggregate in Portland cement-based mortars and concretes. Exteberria et al. [13] observed strength decreases in Portland cement-based concrete using recycled aggregate. The decrease in mechanical properties has also been observed in similar studies [14–15]. By using recycled concrete, it was found that workability decreased and drying shrinkage and water absorption increased by 50% [16]. The fact that the old cement mortar had a porous structure, low density, and high water absorption capacity caused this situation [17]. Despite studies using Portland cement and waste concrete aggregates together, studies in which different sands are used in geopolymer production are limited. Şahin et al. [18] similarly observed strength decreases in geopolymer mortars produced using waste concrete aggregate. However, it is necessary to investigate the reduction of these decreases by using fibers. Although there are disadvantages, recycling of waste concrete makes a significant contribution to the sustainability of the concrete that has completed its life and reduces the need for transport and stacking to the storage area. In this respect, it also contributes to the protection of landfill areas. Thus, it creates a strategic alternative for aggregate resource problems [19]. Basaltic rock aggregate has similar structural characteristics to commonly used limestone aggregate types. Basalt has a hard and dense structure and is a widely available volcanic rock in the world [20]. Basalt aggregates are used in highway and airport pavement construction. It provides high UV and abrasion resistance when used in crushed form. However, it also creates a tight grain structure. While reducing water absorption and abrasion loss rates, it also contributes to the increase of specific gravity [21]. In addition to these properties, there were studies in which it was evaluated as a mineral additive [22–23]. Along with these features, its use in concrete and mortar has brought significant advantages. Şahin et al. [18] showed that basalt aggregate provided a significant increase in the strength of geopolymer mortars, and protected the strength significantly especially under high-temperature effects. As with waste concrete aggregate, increasing this important contribution together with fibers is an important research topic for basalt sand.

Improving the mechanical properties with the effect of fiber brings important advantages. Different types such as carbon, PVA, glass, basalt, woven fabric, and steel fiber have been used in the production of geopolymer [24–26]. Zhang et al. [27–30] produced an alternative product by using nano-SiO_2 and polyvinyl alcohol fibers in the production of metakaolin and fly ash-based geopolymer mortars. When the results were examined, it was seen that the strength and toughness properties increased with the use of PVA fiber and optimum values were obtained between 0.6% and 1% rates. Celik et al. [8] obtained significant values against high temperatures in geopolymer mortars produced with PVA and basalt fibers. Basalt fiber is one of the most used fiber types in concrete and has been evaluated in this study. It is a cost-advantageous, non-toxic, and good insulation fiber obtained by melting basalt rocks at 1400°C. Compared to other fibers, it is cheaper because it does not use additives in its production and requires less energy cost [31–32]. However, it has been observed that it played a role in strength development by contributing significantly to workability. The positive effects of basalt fiber have been confirmed by different authors [33–37]. Also, the effects of this fiber in geopolymer mortars have been studied to a limited extent [38–40]. Ali et al. [38] investigated the effect of basalt fibers and boron waste on reinforced metakaolin-based geopolymer. According to the results, it has been proven that 24 mm BFs have more positive effects than 12 mm. It was observed that the specimens remained stable under freeze–thaw, sulfuric acid effects, and high temperatures.

There are many studies on substitute binder materials in metakaolin-based geopolymer samples. Studies using different fibers and aggregates together are limited. The main objective of this study is to investigate the effects of BF on 100% metakaolin-based geopolymers containing three different aggregates (Rilem, basalt, and recycled waste concrete). Thus, it is aimed to develop the effects of aggregates together with basalt fiber. In this way, the mechanical properties (compressive strength, flexural strength, ultrasonic pulse velocity, density properties), durability properties (abrasion, high-temperature, freeze–thaw) were investigated in the combination of different types of aggregates and basalt fiber.

2. Materials and methods

2.1. Materials

In the study, metakaolin with 97% SiO_2, Al_2O_3, and Fe_2O_3 ratios was used as the binder material. According to the results of preliminary studies, it has been determined that MK can be used as a binder. The specific gravity of the MK used is 2.52. Ground granulated blast furnace slag with a specific gravity of 2.91 was used as pozzolanic material. The chemical compositions of MK and slag are given in Table 1. In geopolymer production, activation of pozzolanic materials is required. This activation process is done using different chemicals. In this study, sodium silicate (Na_2SiO_3) and sodium hydroxide (NaOH) materials with two different alkali properties were used as chemical activators. Three different aggregate types, Rilem sand, basalt sand, and recycled waste concrete, were used separately as the main component in the mixtures. The chemical properties of BS and RWC are given in Table 2. The Rilem sand with a specific gravity of 2.64 is a standard sand variety produced in accordance with EN 196–1 [41]. The main components of the basalt aggregate with a specific gravity of 2.86 are composed of plagioclase minerals, pyroxene group minerals, small amounts of olivine minerals, and opaque minerals as a secondary component. The specific gravity of the recycled waste aggregate is 2.46.

Basalt fiber was used in the geopolymer mortars containing three different aggregate types to examine their mechanical and physical effects. The properties of BF are given in Table 3. The positive effects of BF have been confirmed in cement-based concrete and mortars. The aim of this study is to investigate the effect of BF on metakaolin-based mortars containing different aggregates. When the previous studies were examined, it was seen that the use of 0–1.2% basalt fiber by volume provided significant improvements in the mortar and concrete [8,38]. Based on these studies, four different ratios (0%, 0.4%, 0.8%, and 1.2%) in this range were preferred in this study.

2.2. Mixture design

According to the detailed description of the mixture, firstly the sodium hydroxide solution was prepared as 12 M using distilled water 24 h before the mixture. The solutions were mixed at least 1 h before the mortar mixture so that the sodium hydroxide/sodium silicate ratio of the alkali activator solution was 1/2. These periods were left to cool the solutions. Then, using the stirrer mixer, the activator solution was mixed with metakaolin at a ratio of 1/1 for 1.5 min. In order to increase the calcium content of the mixture and to shorten the setting time, slag was added at 13% by the weight of metakaolin and mixed for a further 1.5 min. Subsequently, the aggregate as 2.25 times the binding material metakaolin was added to the mixture and the mixture was continued for another 1.5 min. In the study, mixtures with MK binder consisted of three groups according to three different aggregate types (RS, BS, and RWC). In the last stage, four different proportions (0%, 0.4%, 0.8%, and 1.2%) of basalt fiber were added to the mixture and the mixture was continued for another 1.5 min. Four different mixtures were produced in each group according to the basalt fiber (BF) ratio. Mixing was completed in a total of 6 min. Then, the mixture was put in molds and subjected to vibration. The mixing procedure is shown schematically in Fig. 1 step by step. Therefore, 12 different mixtures were prepared for all tests. Mix details are given in Table 4. While the use of slag in the prepared mortars provided a hardening period of 2 h, the samples were removed from the mold at the end of this period. Subsequently, the samples were kept at room conditions (at 23 ± 2 °C and 90 ± 5% relative humidity) for 1 day. Before thermal curing, high relative humidity was

Table 1
The chemical compound of the binding materials.

Chemical properties %	SiO_2	Al_2O_3	Fe_2O_3	TiO_2	CaO	MgO	K_2O	Na_2O	L.O.I.
Metakaolin	56.10	40.25	0.85	0.55	0.19	0.16	0.55	0.24	1.11
Slag	40.60	12.83	1.37	0.75	36.08	6.87	0.68	0.79	0.03

Table 2
Chemical composition of basalt sand and recycled waste concrete.

Chemical properties %	SiO_2	Al_2O_3	Fe_2O_3	TiO_2	CaO	MgO	K_2O	Na_2O	L.O.I.
BS	57.9	17.6	8.1	0.9	7.0	2.3	1.9	3.9	0.4
RWC	60.56	0.52	5.82	0.75	12.01	1.83	1.30	2.69	14.52

Table 3
Properties of basalt fiber.

Length (mm)	Diameter (mm)	Specific gravity	Nominal tensile strength (MPa)	Elasticity Module (GPa)
12	0,020	2,73	4100	88

applied as it contributed to strength development and affected shrinkage. The specimens were then put in the oven using a fireproof oven bag. This method contributed to geopolymerization by preventing the evaporation of water in the sample structure. After 72 h curing was applied in the oven at 60 °C, the samples were kept in plastic storage boxes until the test day.

2.3. Test methods

In order to test the compressive strength of different mixtures, cube specimens of 50 × 50 × 50 mm were produced and tested in accordance with ASTM C109 [42]. Geopolymer mortars produced in dimensions of 40x40x160 mm were subjected to flexural strength tests in accordance with ASTM C348 [43]. Prismatic specimens were tested by the three-point flexural method. Flexural and compressive strength tests were carried out for three samples of each series at the end of 7, 28, and 56 days. The results found were calculated by taking the average of three samples. An ultrasonic pulse velocity (UPV) test was performed to determine the ultrasound transmission velocity of specimens obtained from all mixtures. UPV tests were carried out according to ASTM C 597 [44]. 56-day 40x40x160 mm prismatic specimens were used in the UPV test. Three readings were made for each specimen. By taking the arithmetic mean of these three readings, the ultrasound velocity of the specimen was obtained in m/sec.

Abrasion tests of 71x71x71 mm cube specimens produced were carried out in accordance with TS 2824 EN 1338 [45]. The abrasion resistance of the specimens was determined by measuring the weight loss after the test. The porosity ratio of the specimens was determined by measuring the dry and saturated weight of 50x50x50 specimens and then using Archimedes specimens. In order to examine the resistance of geopolymer mortars against high temperatures, the compressive and flexural tests of 50x50x50 mm cube and 40x40x160 prismatic specimens were carried out after 200, 400, 600, and 800 °C temperature effects. In

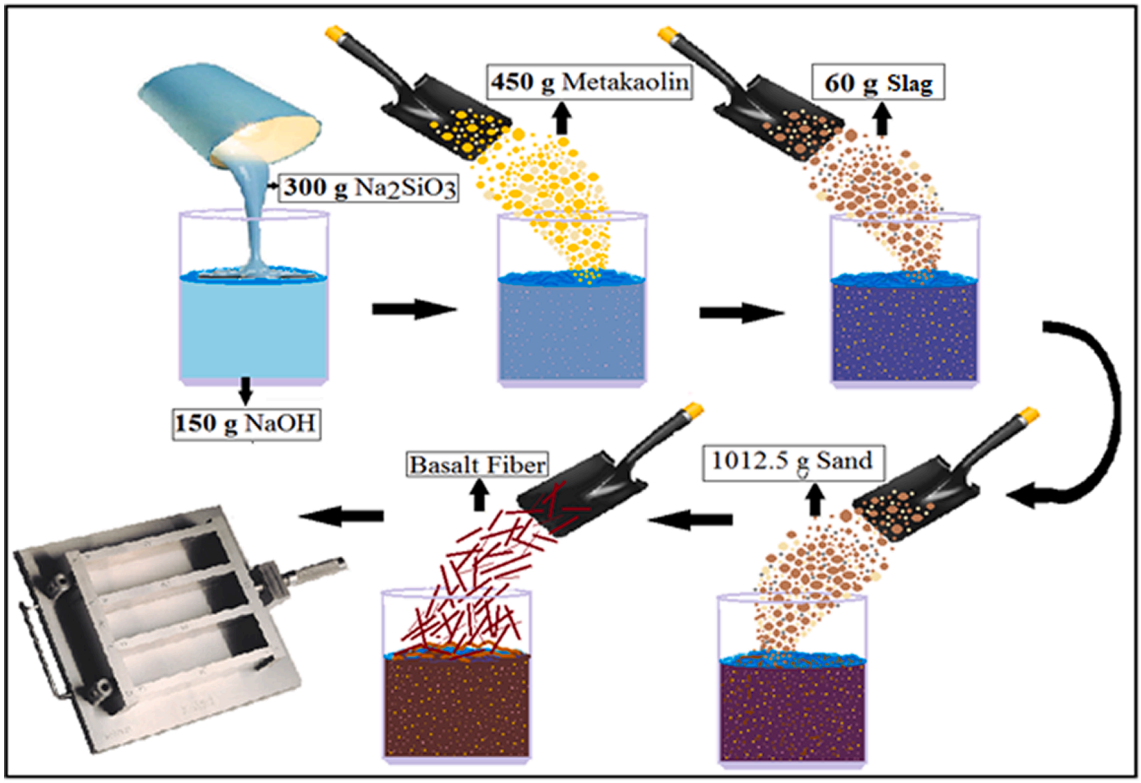


Fig. 1. Steps in the mixing procedure.

Table 4
Mixture content and properties.

No	Mix code	MK (g)	RS (g)	BS (g)	RWC (g)	NaOH(g)	Na_2SiO_3 (g)	Slag (g)	BF (by volume %)
1	RS-BF0	450	1012.5	0.0	0.0	150	300	60	0
2	RS-BF0.4	450	1012.5	0.0	0.0	150	300	60	0.4
3	RS-BF0.8	450	1012.5	0.0	0.0	150	300	60	0.8
4	RS-BF1.2	450	1012.5	0.0	0.0	150	300	60	1.2
5	BS-BF0	450	0.0	1012.5	0.0	150	300	60	0
6	BS-BF0.4	450	0.0	1012.5	0.0	150	300	60	0.4
7	BS-BF0.8	450	0.0	1012.5	0.0	150	300	60	0.8
8	BS-BF1.2	450	0.0	1012.5	0.0	150	300	60	1.2
9	RWC-BF0	450	0.0	0.0	1012.5	150	300	60	0
10	RWC-BF0.4	450	0.0	0.0	1012.5	150	300	60	0.4
11	RWC-BF0.8	450	0.0	0.0	1012.5	150	300	60	0.8
12	RWC-BF1.2	450	0.0	0.0	1012.5	150	300	60	1.2

the high-temperature oven, the temperature rise was set at 5 °C per minute. After reaching the desired temperature, the specimens were kept in the oven at maximum temperature for an additional 1 h. These specimens, which were subjected to high temperature, were allowed to cool down to room temperature in the oven to avoid thermal shock. In this experiment, the physical and mechanical changes of the specimens obtained before and after the temperature were examined and compared. Freeze-thaw effects on 50x50x50 mm cube specimens were investigated. Freeze-thaw tests with 180 cycles were carried out at −18 °C for 12 h and at + 4 °C for 12 h. After the test, the physical and mechanical properties of the specimens were examined before and after freeze–thaw. The abrasion, high-temperature, and freeze–thaw tests were performed after the 56th day.

3. Result and discussion

3.1. Mechanical results

The compressive and flexural strengths of metakaolin-based geopolymers containing three different aggregates and four different ratios of BF were compared in Fig. 2 and Fig. 3, respectively. It was determined that the highest values in terms of both compressive and flexural strength belonged to mixtures containing BS. The most important reason for this was that basalt sand had a dense and durable structure and had a low water absorption rate. Basalt sand had an effect on capillary water absorption, thus reducing the voids ratio and water absorption. While the dense structure prevented the penetration of water, it created a less porous structure. In addition to this situation, the increase in workability together with basalt sand also reflected positively on the strength results. Its low cost and widespread availability increased the strength properties and provided an economic contribution. The results in the literature were also compatible with this situation [46–48]. In the case of using only Rilem sand, lower strength results were obtained compared to basalt sand. Rilem sand didn't directly participate in the geopolymerization reaction and acted as an inert fine aggregate. In this case, it didn't directly affect the strength results [49]. The recycled aggregate effect, on the other hand, caused a significant decrease in compressive strength results compared to the others. Concrete aggregates in the waste condition were aggregates that experienced a loss of strength in their first situation. The effects experienced by waste concrete over the longevity caused a weaker surface formation between paste and aggregate. Despite these situations, progress was achieved in the reactions occurring in the interface transition zone due to the content of calcium hydroxide and its derivatives. When evaluating the structural concrete elements, acceptable results were obtained with the use of recycled aggregate. Besides this, it is seen that it will make a significant contribution to the protection of the environment and sustainability [50–51].

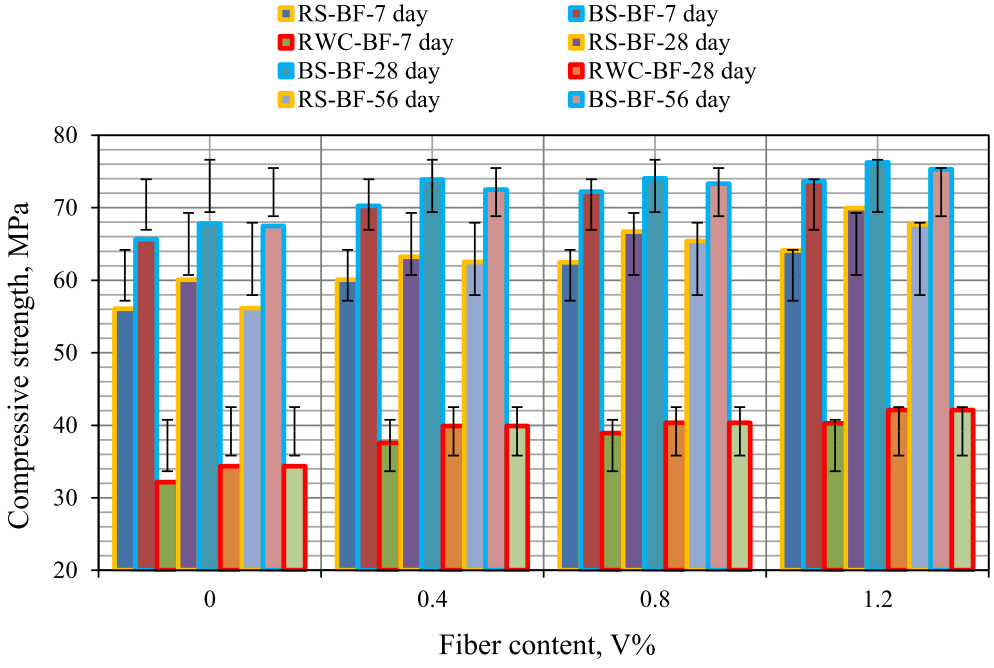


Fig. 2. BF effect on compressive strength of geopolymer specimens.

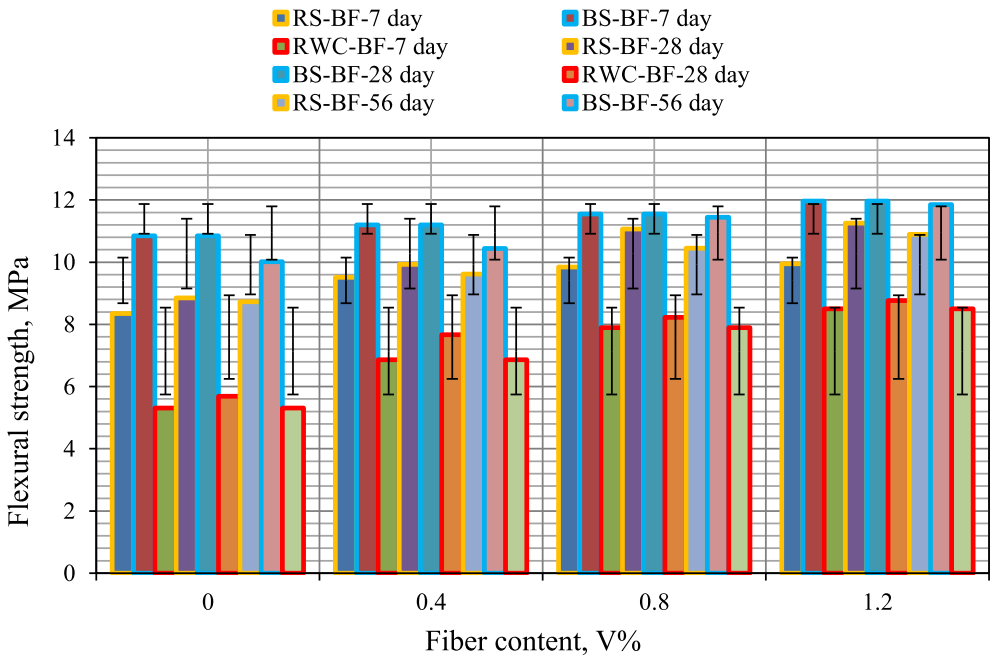


Fig. 3. BF effect on flexural strength of geopolymer specimens.

Strength values of all specimens containing BF increased compared to pure metakaolin-based geopolymer mortars. The addition of basalt fiber had a positive effect on the geopolymeric matrix, resulting in an increase in compressive strength results. Fine and homogeneous distribution of crystal phases played a role in improving the mechanical and physical properties of fibrous materials. The addition of nucleating agents such as ZrO_2, TiO_2, or P_2O_5 was effective in achieving the desired level of microstructure. Although basalt rocks were not needed during the melting process, the production of a naturally obtained nucleator such as Fe_3O_4 contributed in this sense. Thus, nucleating agents have provided a significant advantage over the required fibers [8,38]. The compressive strengths of 56-day-old RS, BS, and RWC filled non-fibrous geopolymer specimens were 56.16, 67.48, and 34.37 MPa, respectively, while fibrous ones of the same mixtures increased up to 67.70, 75.30, and 42.11 MPa, respectively. Although the highest values belonged to mixtures with BS fillings, the highest effect of BF was observed on mixtures containing RWC. According to the results of 56 days, the compressive strength increased by 12% in the BS-filled mixture and 23% in the RWC-filled mixture.

According to the strength results (7, 28, and 56 days), the strength of the sample increased with the increasing age, while decreases were observed. High-temperature curing was effective in this situation. The application of high-temperature curing has brought an important advantage in terms of gaining early strength. While the dissolution in the solid binder material accelerated with the high temperature, the resulting reaction products were also supported. The geopolymerization reaction and thus the strength development was affected by the relationship between heat energy and optimum temperature. The rapid reaction that occurred at the beginning started to negatively affect the reaction products and the microstructure. Puertas et al. [52] stated that diffusion had an effect on geopolymerization and that the reaction products would accumulate near the binder materials. As the dissolution of binding materials, also known as reactive species, increased, the homogeneous microstructure began to leave its place to a heterogeneous and dense structure. The dense structure made diffusion difficult while continuous reactions are reduced. Also, it has been understood that gel chemistry was effective in the geopolymer behavior with age. With the effect of this situation, negative effects were seen on the strength in the following days. But the declines have not been systematic. In other words, increases were seen in addition to the decrease. This situation was due to the compact structure of the geopolymer. Due to its geopolymer compact structure, it managed to turn the decreases into an increase over time [18,53]. If the situation was summarized, it was seen that a certain value was preserved even though sudden changes were observed between 7, 28, and 56-day strength results with the effect of high temperature.

Also, flexural strength and compressive strength behaved similarly. Flexural strengths typically increased with increasing BF ratio in all mixtures (Fig. 3). So, basalt fibers have shown their effect on flexural strength. It significantly reduced the cracks that occurred during the bending test by transferring the load more efficiently. In other words, it slowed down the crack development by redistributing the resulting stress. Thus, it had a significant effect on flexural strength [8,38]. Maximum flexural strength was obtained as 11.97 MPa for the BS-filled mixture containing 1.2% BF. Compared to other aggregates, the BF effect was more pronounced on RWC filled mixtures. According to the results of 56 days, the flexural strength of the geopolymer sample containing fiberless-RWC was 5.31 MPa and the strength of the sample containing 1.2% BF from the same mixture was 8.50 MPa.

3.2. *UPV test results*

The main parameter that determines the quality of concrete and mortars is compressive strength. Ultrasonic pulse velocity test is an important parameter that can be used to ensure the results obtained in compressive strength results non-destructively. Therefore, in this study, the UPV test was used to non-destructively investigate the effect of basalt fiber with different content ratios and different aggregates in the geopolymeric matrix continuity. The 56-day UPV test results are given in Fig. 4.

While there is a reciprocal proportion between the number of voids and the wave velocity in the material structure, it is seen that the relationship between the unit weight and the wave velocity is important. The penetration ratio is found by calculating the ratio of the distance the sound waves will go between the source point and the receiver to the elapsed time [8,46]. When the matrix structure has more voids, it will increase the required time and cause a decrease in the coefficient of ultrasonic sound penetration ratio. Therefore, the voids ratio is a

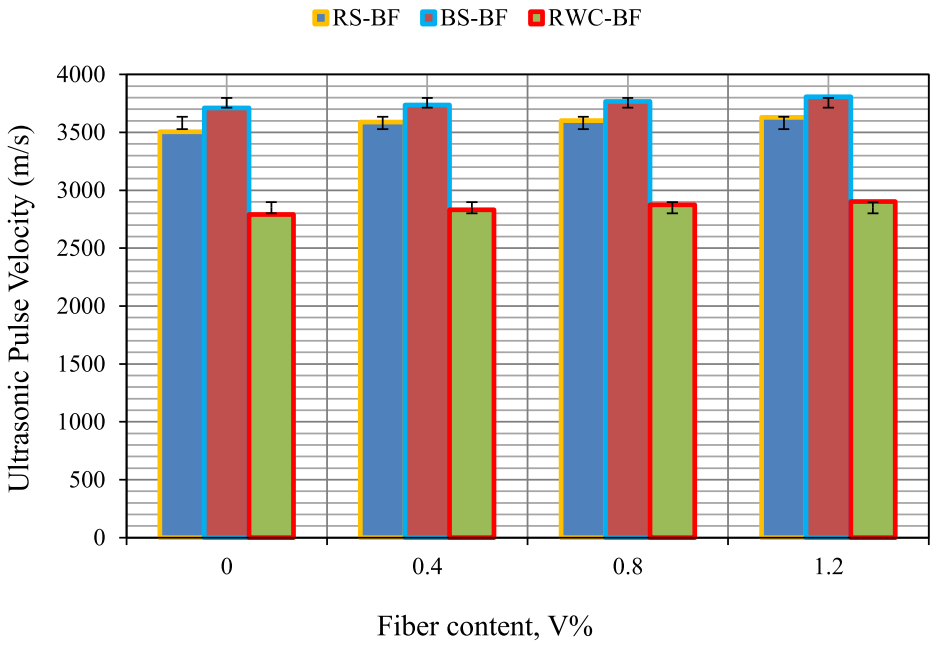


Fig. 4. BF effect on the UPV values of geopolymer specimens.

significant factor affecting the mechanical properties of geopolymer samples.

These situations played a role in the UPV results obtained by using different types of aggregates. While the voids ratio was higher in the RWC with the lowest unit weight, the basalt sand with the highest unit weight had the lowest voids ratios. Especially, the UPV results of RWC-filled mortars were lower than the others. Positive effects of BF on UPV results were observed for all three aggregate-filled mortars. However, when the BF ratio of BS-filled mortars was 0.8%, the UPV value was 3768 m/s and the UPV value increased to 3807 m/s when the BF ratio was 1.2%. Although the fiber effect increased the UPV results by decreasing the voids ratio, this increase was not at a high rate. This was due to the fact that the effect of the fibers didn't directly affect the matrix homogeneity and compactness. Although the maximum UPV values belong to mortars filled with RS and BS, the highest effect of BF was observed in mortars filled with RWC. The UPV value in RWC-filled mortars increased from 2792 m/s to 2903 m/s.

3.3. Porosity ratios

To determine the number of voids that the geopolymer samples had, porosity ratios were determined. The porosity ratios of geopolymer mortars containing different phases are given in Fig. 5. Depending on the type of sand, porosity ratios vary. The fact that the unit weight of basalt sand was higher and had a dense structure has made it the lowest porosity ratio. The lower unit weight of Rilem sand increased the porosity ratio [18]. Although the porosity ratios of RS and BS-filled mortars were close to each other, they were lower compared to RWC-

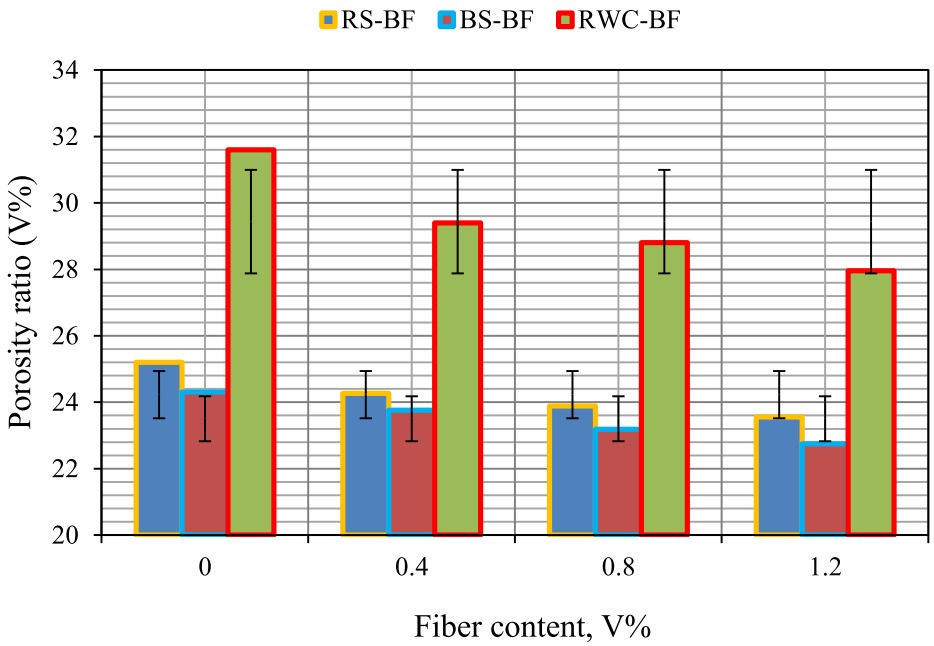


Fig. 5. BF effect on porosity ratio of geopolymer specimens.

filled mortars. The use of recycled aggregate led to a significant increase in porosity ratio due to the low unit weight of RWC aggregates. In this case, the main factor was the high porosity of the waste concrete aggregates attached to the mortars and their potential as a channel to help water transport in the matrices. Also, the age of RWC aggregates was effective. Since recycled aggregates obtained from waste concrete contained aged paste, they cannot be as dense as natural aggregates. These pores combined with the pores in the geopolymer mortars and reduced the density of the produced composite [50,52]. It was observed that the results were parallel with the UPV and mechanical results. Average porosity ratios of RS, BS, and RWC-filled mortars were obtained as 24.23%, 23.50%, and 29.44%, respectively. With the addition of BF, the porosity ratio of all mixtures was reduced. Since fiber reinforcement caused the geopolymer samples to behave more systematically and slightly increased the unit weight, resulting in a slight increase in the porosity ratio [38]. As with other results, BF most affected the porosity ratio of RWC-filled mortars. The porosity ratio in RWC-filled mortars decreased by 12% from 31.6% to 27.96%, with the addition of 1.2% BF.

3.4. Abrasion results

The abrasion results of the 56-day specimens are summarized in Fig. 6. In all three mortar groups with RS, BS, and RWC filling, the highest weight loss due to abrasion was observed in those without fiber. It was also seen from Fig. 6 that the highest weight loss belonged to RWC-filled mortars. This difference between the abrasion results of RWC and BS-filled mortars was due to the abrasion properties of RWC and BS aggregates. Abrasion resistance of geopolymer composites was significantly affected by curing conditions, mix content properties, and raw material properties [54–55]. According to the Los Angeles test results in the literature, the abrasion of BS was 16% while the abrasion of RWC was 38% [56]. According to the literature, when RWC was used in cement-bonded concretes, it has been determined that 18–22% weight loss was observed [57]. It was determined that the lowest weight loss belonged to the BS-filled mortar. The harder structure of the basalt sand was effective in this case. In addition, the increase in the capillary water absorption ratios also decreased the abrasion resistance in RWC aggregates [18]. BS-BF1.2 was found to be the most resistant to abrasion with a weight loss of 12.02 g. According to the results of this study, the use of mineral additives showed the abrasion resistance of geopolymer mortars [46]. For all mixtures, with increasing BF, the weight loss has been decreased with a slight slope. It was understood that there was a parallel relationship between abrasion results and mechanical strength. According to the literature [46] it has been stated that the abrasion resistance of concrete was directly related to its strength. When Fig. 5 and Fig. 6 were compared, it was understood that there was also a direct relationship between abrasion results and porosity results. Therefore, the amount of fiber used was important to reduce the porosity ratio, which significantly affected the abrasion. The inverse relationship between the abrasion-porosity results and the mechanical-UPV results strengthened the accuracy of the data.

3.5. High-temperature test results

In this section, the behaviors of 56-day geopolymer specimens, obtained from twelve different mixtures, have been investigated between room temperature and 800°C temperature. Compressive, flexural, UPV, and weight loss results after high temperature are compared in Figs. 7-10. There was no significant change in the compressive and flexural strength (Fig. 7 and Fig. 8) of the specimens at 200°C, but after 400°C, there was a significant decrease in the strength of the specimens at high temperatures. Maximum compressive and flexural strengths belonged to BS-BF mixtures. It was observed that the minimum values belonged to RWC-BF. In the study of Tanyildizi and Yonar [58] the compressive strengths of geopolymer mortars exposed to high temperatures in the range of 200–800 °C have been obtained as 10–45 MPa. In this study, minimum compressive strength was obtained as 8.5 MPa for RS-BF0 (800°C) and maximum compressive strength as 66.47 MPa for BS-BF1.2. The compressive and flexural strengths of RS-BF0.4 at 600 °C were 28.84 MPa and 1.75 MPa, respectively, while the compressive and flexural strengths of RWC-BF0.4 were 18.23 MPa and 0.94 MPa. Generally, BF had a positive effect at high temperatures ranging from 200 to 800 °C. While the compressive strength of BS-BF0 at 200 °C was 58.17 MPa, the compressive strength of BS-BF0.4 after 200 °C was 62.25 MPa. The biggest impact of BF was on mortars exposed to 200 °C. The biggest effect of BF was in RWC-filled mortars exposed to 200 °C temperature. The compressive and flexural strengths of RWC-BF0 at 200 °C were 38.99 MPa and 2.26 MPa, respectively, while those of RWC-BF1.2 increased to 45.16 MPa and 3.61 MPa. An average of 7.5% increase was observed in the compressive strength of RWC-BF mortars exposed to

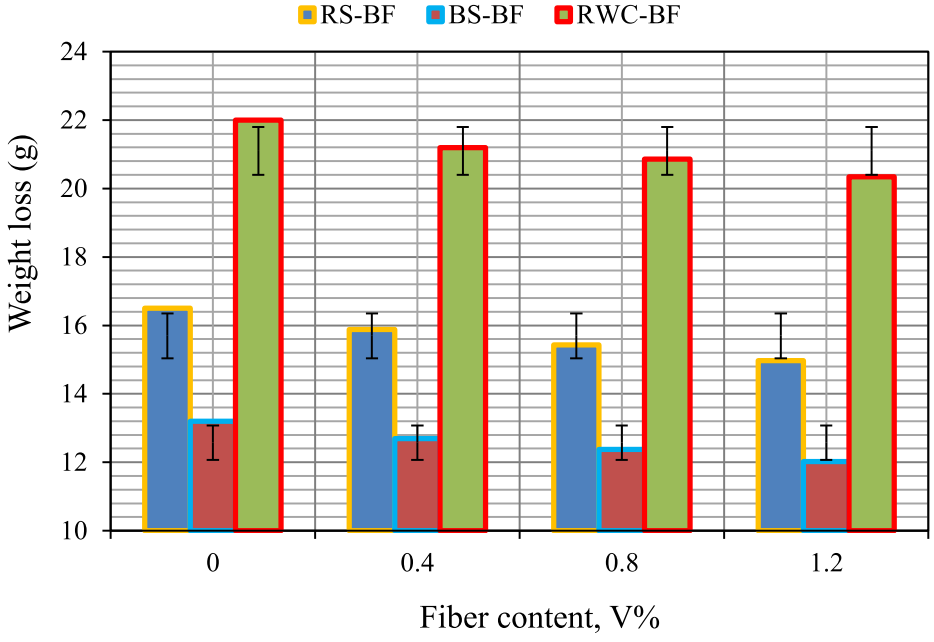


Fig. 6. BF Average weight loss due to abrasion.

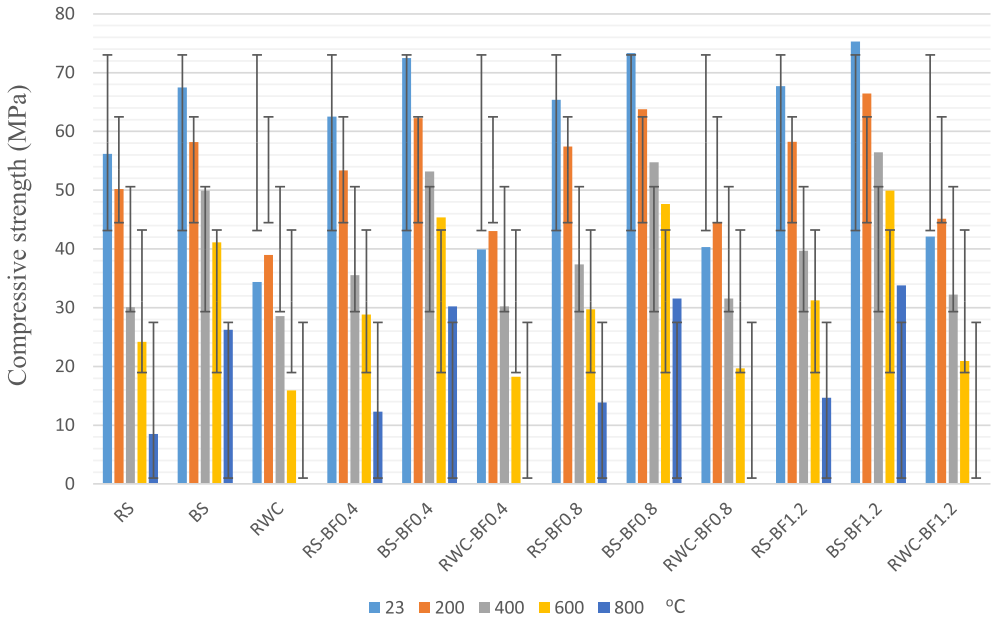


Fig. 7. Compressive strength of geopolymer specimens after high temperature.

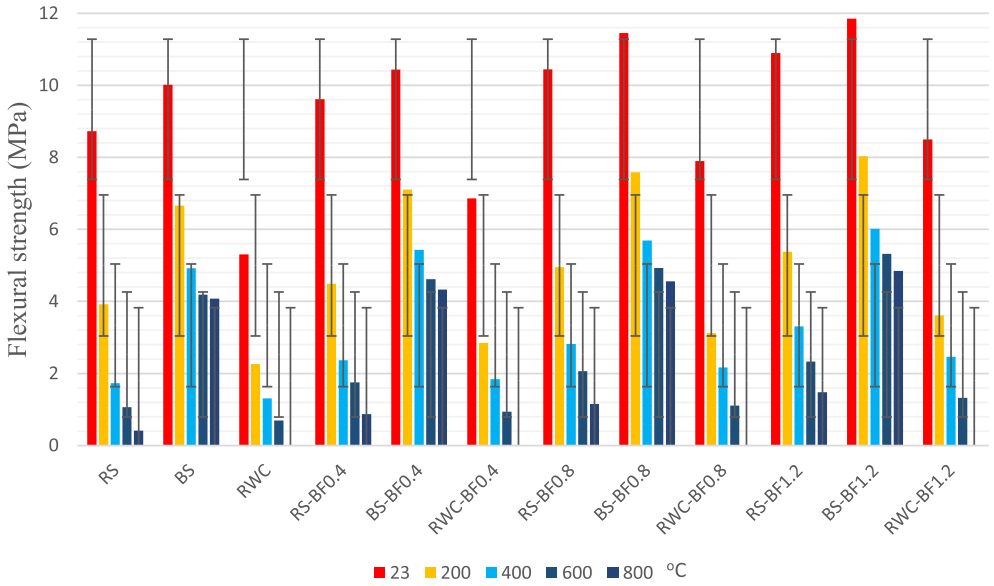


Fig. 8. Flexural strength of geopolymer specimens after high temperature.

200 °C, then the strength decreased as the temperature increased. The same behavior was observed at 200–300 °C temperatures in conventional concretes [59]. Although the strength of RWC-filled mortars increased up to 200–300 °C, the specimens were not tested after 800 °C due to sudden disintegration. The reason for this situation may be the internal evaporation of RWC aggregates in addition to the evaporation in the paste. Therefore, tests of RWC filled mortars exposed to 800 °C could not be performed. According to the literature, the same situation occurred in RWC-filled cement-based concrete after 800 °C temperature [59].

According to the literature, it has been reported that the strength of geopolymer composite exposed to high temperatures depended on the activator/binder ratio, the activator type, the curing temperature, and the raw material used [58,60–61]. When geopolymer mortars were exposed to high temperatures, the free water in the matrix evaporated and the strength decreased due to dehydration [38,53,62]. Evaporation in the matrix caused internal pressure generation. The steam pressure increased with the increase in temperature. After the internal pressure reached a certain limit, the resistance of composite against thermal effects decreased and caused cracks on the surfaces. Also, high temperatures created micro-cracks in the interface transition area between aggregate and paste, creating thermal incompatibilities [63]. At the end of these situations, there was a loss of weight and thus a decrease in strength. Another reason for the formation of microcracks was crystallization in the internal structure. This situation negatively affected strength and ductility. Al SiO gel structure in geopolymer mortars underwent more crystallization at higher temperatures [64]. Also, in this case, micro cracks and developing pores seriously affected the flexural strength. In Fig. 9, weight loss was observed especially after 400°C temperature. Typically, weight loss in geopolymer mortars was due to three reasons. The first was the physical weight loss due to the evaporation of absorption water at the 30–210 °C temperature range. In the second step, deterioration of the side chains at the temperature range 210–400 °C caused the weight loss. The weight loss in the third stage

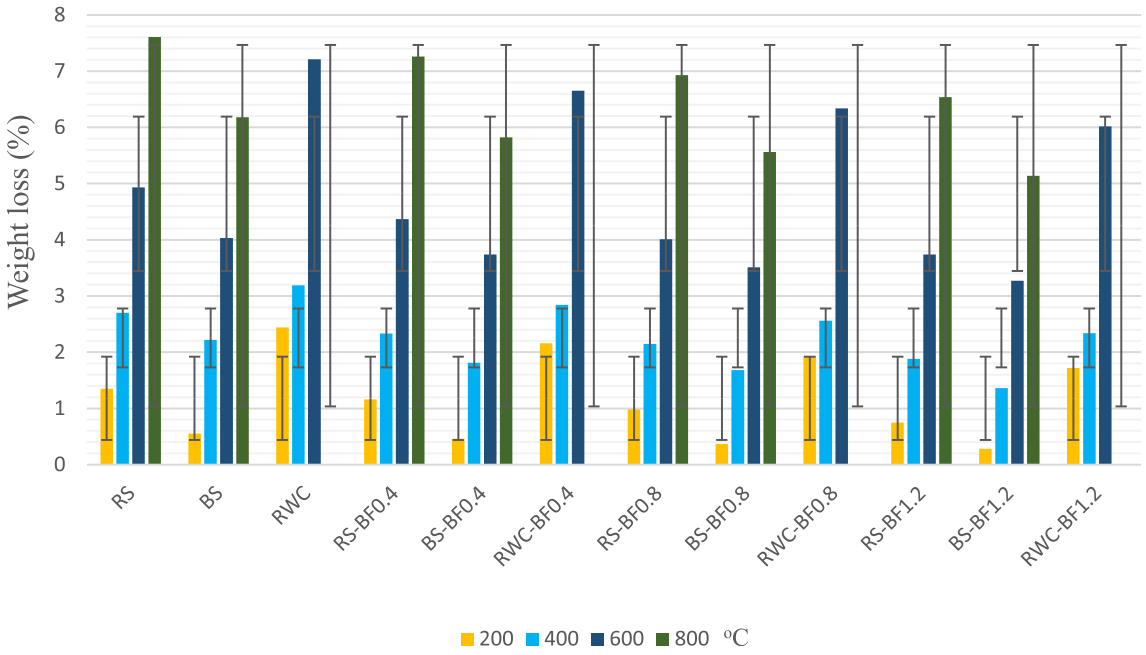


Fig. 9. Weight loss after the high temperature in geopolymer specimens.

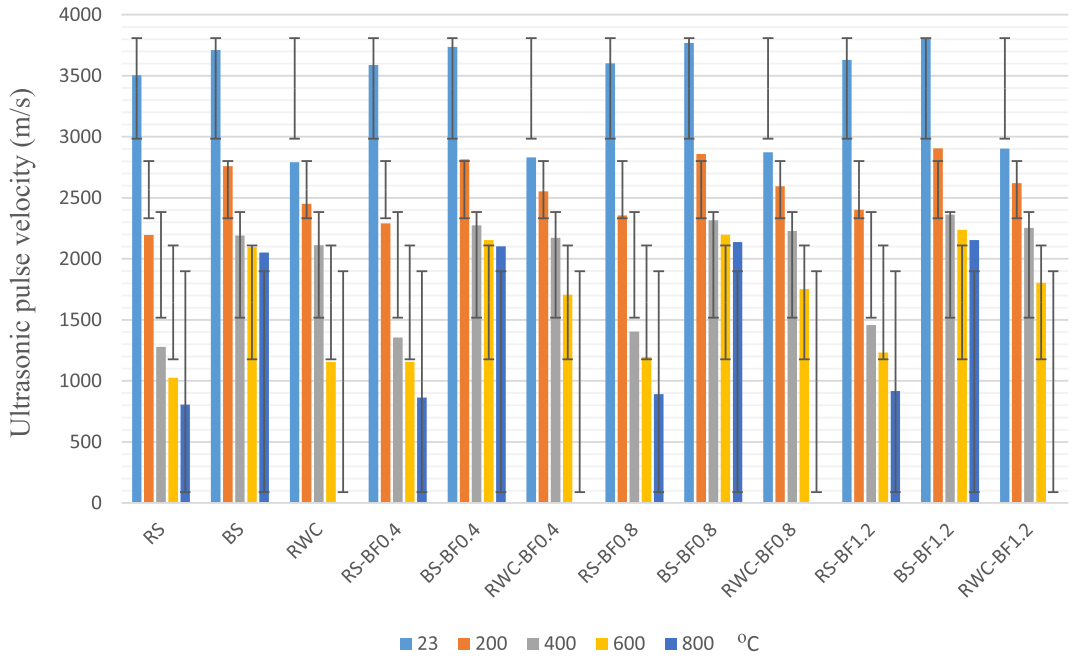


Fig. 10. UPV values after high temperature.

was due to the degradation of the main polymer chains at 400–500 °C. In addition, the weakening of the bond between aggregate and paste at high temperatures increased weight losses [65–66]. As shown in Fig. 9, the lowest weight loss occurred in BS-filled mortars. Also, the highest weight loss occurred in RWC-filled mortars. The weight loss of RWC-filled mortars after 800°C was not calculated due to the dispersion of the specimens. Since BS-filled geopolymer mortars had a denser structure, thermal conductivity was high in these mortars. Therefore, fewer thermal reactions and weight loss occurred in these mortars [67]. In addition, during the formation of BS, products such as Fe_3O_4, which were resistant to high temperatures above 800°C, were formed and gained strength [8]. The addition of BF reduced the weight loss results.

When the UPV results were examined, it was seen that the values were parallel with the strength results (Fig. 10). Before exposure to high temperature, the highest UPV values have been obtained for BS-BF mortars. This was because, as stated in the strength description, these mortars were denser and had high continuity. The effect of BF on UPV results was low. However, it was observed that UPV values increased with the increase of BF in RWC-BF at temperatures of 23–200 °C. The UPV value of RWC-BF0 exposed to 200°C was measured as 2451 m/s, while that of RWC-BF1.2 was measured as 2621 m/s. After 800°C temperature, UPV values of RWC-BF samples could not be obtained due to their disintegration. UPV values decreased as the temperature increased in all mortars. The reason for this situation was that the pore size increased and the continuity decreased due to evaporation in the internal structure [68]. The pores formed in the inner structure of the

geopolymer also caused the polycondensation reaction of geopolymerization to slow down [69].

To examine the specimen structure after high temperature, SEM analysis of specimens containing three different aggregates after 800°C was performed. SEM images of RS-BF1.2, BS-BF1.2, and RWC-BF1.2 are given in Fig. 11. When SEM images were examined after 800°C, it was seen that the fibers were melted. Here, the good interfacial bonding of the fibers before high temperature contributed to the behavior after the temperature. In addition, it helped to evacuate the water vapor after the high-temperature effect by creating escape points in the sample with voids in proportion to its volume with its melting. Along with this, it helped to maintain stability. As stated in the literature, it decreased the vapor pressure formed in concrete and mortar by melting at high temperatures. Thus, they also reduced the piece throwing behavior during heating. Along with the fiber effect, the aggregate types used were also effective [8].

In addition, it will be seen that the most micro-cracks and air voids were in the RWC-filled sample, while the RS-filled sample had fewer air voids and micro-cracks, and the basalt sand-filled sample was affected the least after 800°C. When the images were examined, it was observed that air voids started to form with the microcrack progression in the specimen with RWC. It was observed that the stability of the microstructure in this sample was lost. The main reasons were phase transformation, weight loss, and matrix decomposition. These situations caused structural defects and then intensified the defect formation. Thus, the structure became more porous. This situation caused deterioration in the sample after 800°C temperature. Nevertheless, the metakaolin-based geopolymer specimens retained their stability in other sand types and especially in the BS-added specimen. This has been confirmed by the literature [70]. Post-high temperature microstructure behavior was most likely related to the hardness and density of the aggregate.

3.6. Freeze-thaw test results

The compressive and flexural strength results of the 56-day geopolymer specimens exposed to 180 cycles of freeze–thaw effect are given in Figs. 12 and 13, respectively. After the freeze–thaw effect, the compressive strength of RS, BS, and RWC-filled mortars without fiber increased by 10%, 19%, and 16%, respectively. It was noteworthy that the compressive strengths obtained after the freeze–thaw test increased compared to before the test. These results in the study were in parallel with previous studies. According to the studies in the literature, freeze–thaw caused either ineffective or slight strength increase on geopolymer mortars. In the study of Yunsheng et al. [70] it was stated that the reason for the increase in the strength of geopolymer composites after freeze–thaw was related to the addition of slag and the increase in its ratio. In other words, the formation of geopolymer composites with dense structures due to the slag used and the continuation of the production of geopolymeric products during freeze–thaw were the main reasons for the increase in strength. The good adhesion degree and compact structure of the geopolymer matrices were also effective in this situation. Thus, freeze–thaw cycles acted as the continuation of the curing process of geopolymers, creating a progress process in the matrix. Similarly, the reason for the strength increase occurring after freeze–thaw was explained in the study of Puertas et al. [71]. It was stated that mortar reached its final strength by continuing slag activation due to high humidity conditions under the effect of freeze–thaw. The void ratio, void geometry, void dimension, and distribution significantly affected the strength of mortar after freeze–thaw. Water ratio in the mortar's internal structure, degree of saturation, freezing rate, and curing conditions were other factors affecting the strength [46]. Therefore, in order to increase the resistance of mortar against freeze–thaw, it was important to reduce the porosity ratio in its internal structure. Using the optimum amount of mineral additives played an important role in the development of this feature [72–73]. The

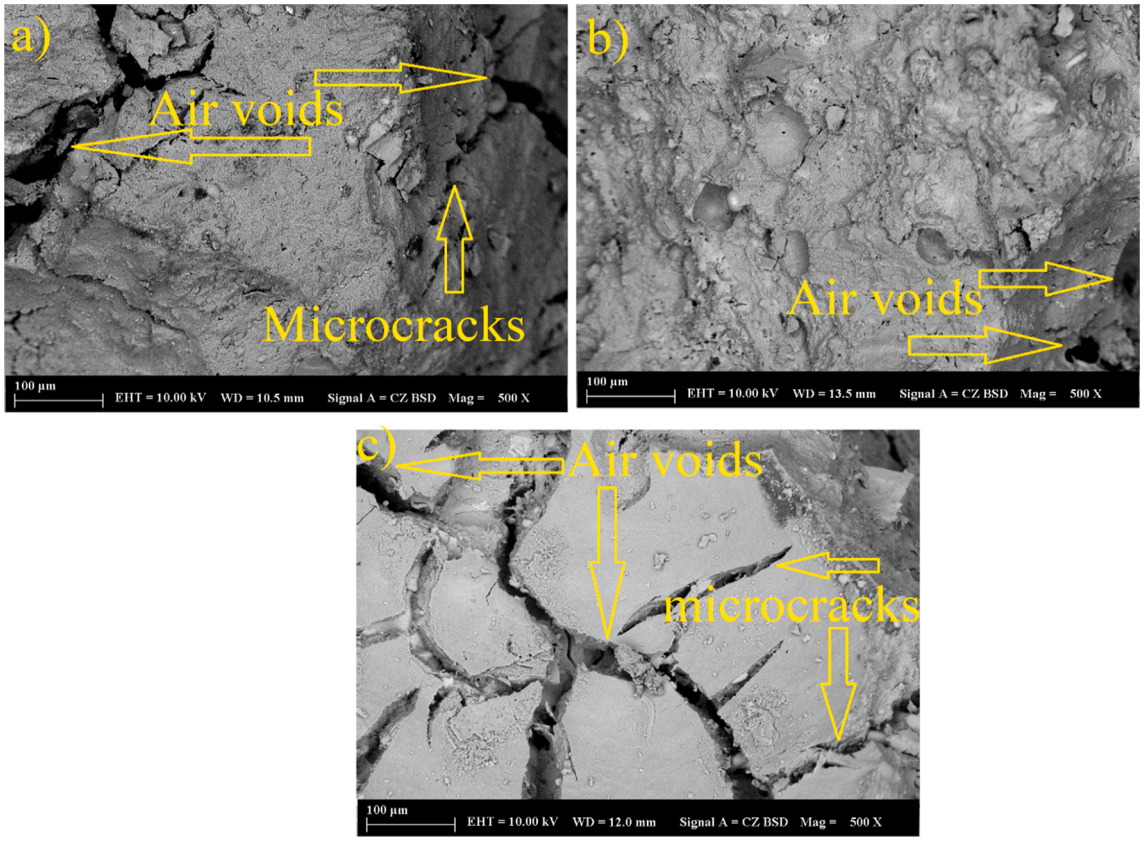


Fig. 11. SEM images of specimens containing RS-BF1.2 (a), BS-BF1.2 (b) and RWC-BF1.2 (c) after 800 °C.

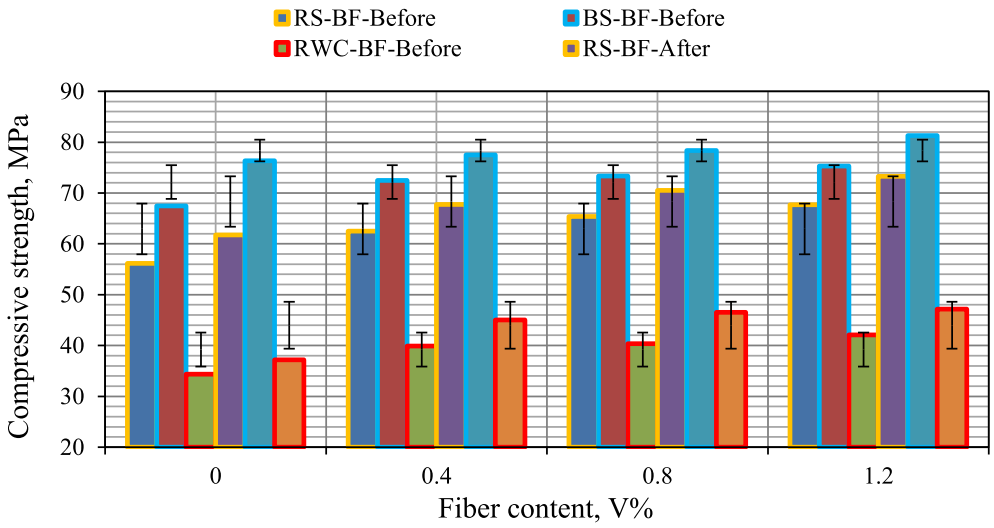


Fig. 12. Freeze-thaw effect on compressive strength of geopolymer containing BF and different aggregates.

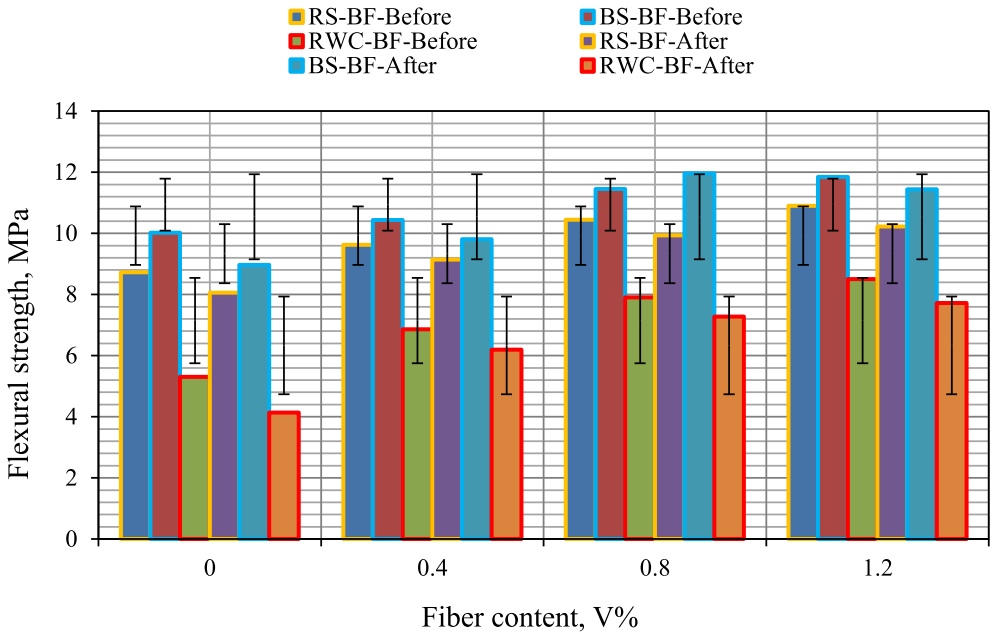


Fig. 13. Freeze-thaw effect on flexural strength of geopolymer containing BF and different aggregates.

important role of MK, slag, BF and different sands used in the study in increasing the freeze–thaw resistance has been confirmed.

Basalt fiber had a positive effect on the strength of all three aggregate-filled mixtures exposed to the freeze–thaw effect. Maximum strength results were obtained for mortars containing 1.2% BF. Also, the most positive effect of BF was observed on RWC-filled mortars. Compared to non-fibrous mortars, the compressive strength of RS-BF, BS-BF, and RWC-BF mortars increased by 19%, 7, and 27%, respectively, after freeze–thaw. Likewise, the flexural strengths of the same mixtures increased by 27%, 28%, and 87%, respectively. As shown in Fig. 13, unlike compressive strength results, flexural strengths decreased after freeze–thaw. The main reason for this situation was the formation of cracks parallel to the load applied in the flexural test. The changes in the weight of the specimens after the freeze–thaw cycles are given in Fig. 14. The weight of all mixtures increased slightly after the test. Microcracks occurred in specimens during freeze–thaw. Meanwhile, the moist environment entered the cracks and caused the weight of the specimen to increase. Maximum weight increase occurred in RWC-filled mortars and minimum weight increase occurred in BS-filled mortars. This means that the number of microcracks formed in RWC-filled mortars during freeze–thaw was higher. Also, weight gain decreased significantly with the addition and increasing ratio of BF. This was important because the addition of BF prevented the development of microcracks, resulting in fewer pores after freeze–thaw. The weight changes of RS-BF1.2, BS-BF1.2, and RWC-BF1.2 mortars decreased as 47%, 56%, and 50%, respectively, compared to non-fibrous. As a result, considering Fig. 14, if the specimens were subjected to a greater number of freeze–thaw cycles, the resulting microcracks may cause greater damage.

SEM images of RS-BF1.2, BS-BF1.2, and RWC-BF1.2 obtained after 180 cycles of freeze–thaw are given in Fig. 15. The water in the mortar caused the material to crystallize. This situation led to the formation of fine cracks in the mortar. The crystal structure of the layer-like products on the geopolymer surface can be seen in BS added mortar. The SEM image of RWC-filled mortar contained more porosity than microcracks compared to others. This can also be noticed by the high conductivity of

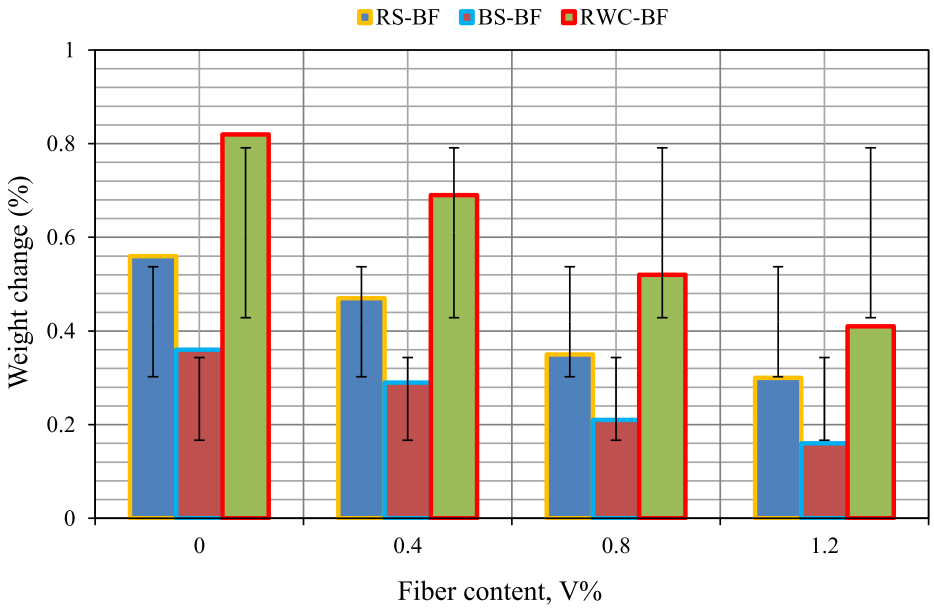


Fig. 14. Weight change after freeze–thaw.

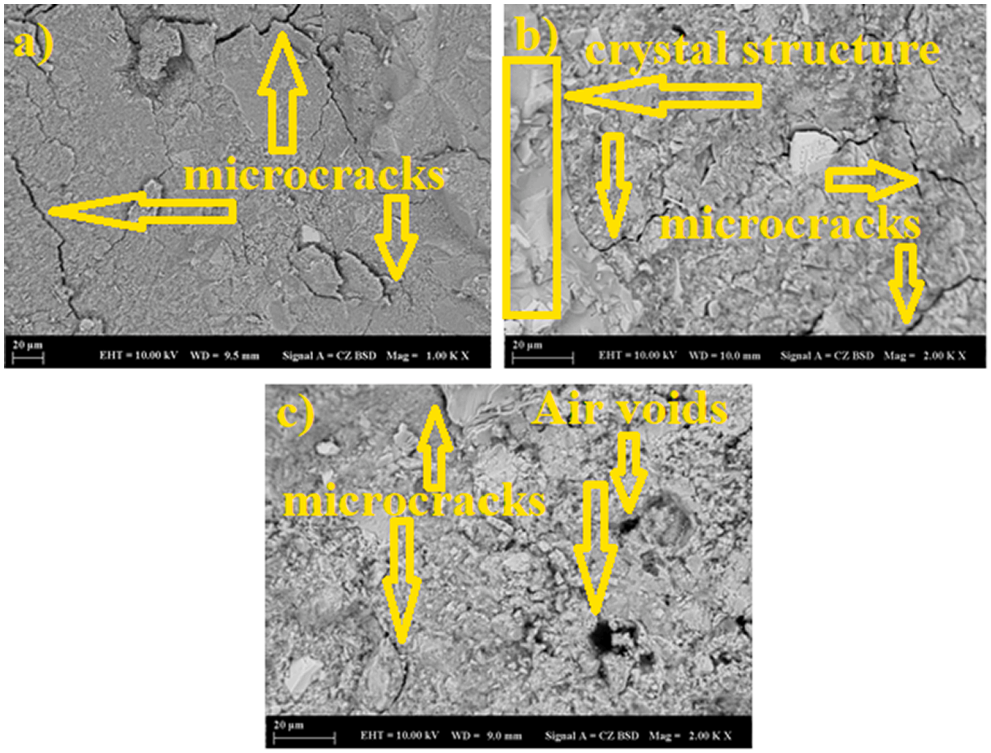


Fig. 15. SEM images of specimens containing RS-BF1.2 (a), BS-BF1.2 (b) and RWC-BF1.2 (c) after freeze–thaw.

the moisture coated in the voids. However, as in the literature, disintegration and fragmentation in the microstructure after freeze–thaw was not observed in all three metakaolin-based geopolymers [74]. The slow development of cracks in geopolymer composites kept the specimen stable. Therefore, when geopolymer composites were exposed to freeze–thaw for even 300 cycles, the strength didn't decrease [62]. It was known that metakaolin-based geopolymers were resistant to freeze–thaw from both cement mortars and other geopolymers such as fly ash-based. In the study of Zhao et al. [75] 1–2 μm wide cracks were formed in the structure of the fly ash-based geopolymer after 125 cycles of freeze–thaw. These cracks caused a significant reduction in strength, unlike MK-based geopolymers. After 225 cycles, the crack width increased to 2–4 μm and caused the integrity of the structure to be destroyed by connecting and forming a network. Also in cementitious mortars, after 225 cycles, the defects were less than fly ash-based geopolymers, but the hydration products in the structure were observed to have weak peeling.

4. Conclusions

In this paper, the performance of basalt fiber reinforced metakaolin-based geopolymer samples by using Rilem, basalt, and recycled waste

concrete aggregates were investigated:

- When the mechanical and physical properties were examined, it was seen that the highest results were found with basalt sand. The dense and hard structure of basalt sand ensured that the geopolymer matrix had a tight grain structure. With the higher unit weight of basalt sand, higher strength and UPV results were obtained, while a lower porosity ratio occurred. By using Rilem sand, the unit weight effect was weakened, while acting more as an inert fine aggregate reduced the results. In the case of using recycled waste concrete aggregates, the effect of the decrease in the unit weight value was reflected. The effects experienced during its longevity led to the formation of a weaker aggregate and paste interface. Despite this, the reaction progressed due to the calcium hydroxide and its derivatives contained in the recycled aggregates. Thus, while achieving acceptable results for structural elements, it also contributed to sustainability. The addition of basalt fiber provided a more systematic performance due to the fine and homogeneous distribution of the crystal phases. In addition, due to the Fe_3O_4 nucleator obtained naturally during its melting, fiber contributed to the desired level of microstructure. According to the results, BF had positive effects, especially when 0.8–1.2% was used.
- When the strength results are examined between 7, 28, and 56 days, increases, as well as decreases, were observed. The main reason for this situation was the application of high-temperature curing. While high-temperature curing accelerated the reactions in the early period, it caused early strength gain and transformed the homogeneous structure into a heterogeneous and dense structure. Because of this situation, continuous reactions decreased in the following periods. Thus, the negative effects began to be seen. But the declines were not systematic. The compact structure of the geopolymers also provided an increase despite the decreases.
- When the behavior of the geopolymer samples was examined at the end of the durability tests (high temperature, freeze–thaw, and abrasion test), it was seen that the results were generally compatible with the 56-day results. In this case, the compact structure of the geopolymer played a role. At the end of the tests, the geopolymer samples preserved their stability. Only waste concrete aggregate lost its stability after 800°C. SEM analyzes also confirmed the results obtained.

Declaration of Competing Interest

The authors declare that they have no known competing financial interests or personal relationships that could have appeared to influence the work reported in this paper.

Acknowledgment

This work was supported by the research fund of the Yildiz Technical University, the authors would like to express their sincere gratitude to the scientific research coordination unit for their financial support to the project (Project number: FBA-2019-3558).

References

[1] Q. Tang, Y. He, Y.-P. Wang, K.-T. Wang, X.-M. Cui, Study on synthesis and characterization of ZSM-20 zeolites from metakaolin-based geopolymers, Appl. Clay Sci. 129 (2016) 102–107.
[2] A.A. Arslan, M. Uysal, A. Yılmaz, M.M. Al-mashhadani, O. Canpolat, F. Şahin, Y. Aygörmez, Influence of wetting-drying curing system on the performance of fiber reinforced metakaolin-based geopolymer composites, Constr. Build. Mater. 225 (2019) 909–926.
[3] H. Wang, H. Li, F. Yan, Synthesis and mechanical properties of metakaolinite-based geopolymer, Colloids Surf., A 268 (1–3) (2005) 1–6.
[4] A.M. Rashad, Metakaolin as cementitious material: History, scours, production and composition–A comprehensive overview, Constr. Build. Mater. 41 (2013) 303–318.
[5] X.-M. Cui, L.-P. Liu, G.-J. Zheng, R.-P. Wang, J.-P. Lu, Characterization of chemosynthetic Al_2O_3–$2SiO_2$ geopolymers, J. Non-Cryst. Solids 356 (2) (2010) 72–76.
[6] O. Biel, P. Rożek, P. Florek, W. Mozgawa, M. Król, Alkaline activation of kaolin group minerals, Crystals 10 (4) (2020) 268.
[7] M. Uysal, M.M. Al-mashhadani, Y. Aygörmez, O. Canpolat, Effect of using colemanite waste and silica fume as partial replacement on the performance of metakaolin-based geopolymer mortars, Constr. Build. Mater. 176 (2018) 271–282.
[8] A. Celik, K. Yilmaz, O. Canpolat, M.M. Al-Mashhadani, Y. Aygörmez, M. Uysal, High-temperature behavior and mechanical characteristics of boron waste additive metakaolin based geopolymer composites reinforced with synthetic fibers, Constr. Build. Mater. 187 (2018) 1190–1203.
[9] P.L. Maier, S.A. Durham, Beneficial use of recycled materials in concrete mixtures, Constr. Build. Mater. 29 (2012) 428–437.
[10] S. Marinković, J. Dragaš, I. Ignjatović, N. Tošić, Environmental assessment of green concretes for structural use, J. Cleaner Prod. 154 (2017) 633–649.
[11] F. Faleschini, M.A. Zanini, C. Pellegrino, S. Pasinato, Sustainable management and supply of natural and recycled aggregates in a medium-size integrated plant, Waste Manage. 49 (2016) 146–155.
[12] G. Dobbelaere, J. De Brito, L. Evangelista, Definition of an equivalent functional unit for structural concrete incorporating recycled aggregates, Eng. Struct. 122 (2016) 196–208.
[13] M. Etxeberria, E. Vázquez, A. Marí, M. Barra, Influence of amount of recycled coarse aggregates and production process on properties of recycled aggregate concrete, Cem. Concr. Res. 37 (5) (2007) 735–742.
[14] K.K. Sagoe-Crentsil, T. Brown, A.H. Taylor, Performance of concrete made with commercially produced coarse recycled concrete aggregate, Cem. Concr. Res. 31 (5) (2001) 707–712.
[15] S.W. Tabsh, A.S. Abdelfatah, Influence of recycled concrete aggregates on strength properties of concrete, Constr. Build. Mater. 23 (2) (2009) 1163–1167.
[16] S. Marinković, V. Radonjanin, M. Malešev, I. Ignjatović, Comparative environmental assessment of natural and recycled aggregate concrete, Waste Manage. 30 (11) (2010) 2255–2264.
[17] M.S. De Juan, P.A. Gutiérrez, Study on the influence of attached mortar content on the properties of recycled concrete aggregate, Constr. Build. Mater. 23 (2) (2009) 872–877.
[18] F. Şahin, M. Uysal, O. Canpolat, Systematic evaluation of the aggregate types and properties on metakaolin based geopolymer composites, Constr. Build. Mater. 278 (2021), 122414.
[19] A. Akbarnezhad, Z.S. Moussavi Nadoushani, A computational method for selection of optimal concrete recycling strategy, Mag. Concr. Res. 67 (11) (2015) 543–558.
[20] D. Constantiner, S. Diamond, Alkali release from feldspars into pore solutions, Cem. Concr. Res. 33 (4) (2003) 549–554.
[21] H. Maiah, G. Al-Khateeb, Effect of basalt and limestone aggregate combinations on Superpave aggregate properties, The 5th Jordanian International Civil Engineering Conference, At Amman, Jordan, 2012.
[22] L. Laibao, Z. Yunsheng, Z. Wenhua, L. Zhiyong, Z. Lihua, Investigating the influence of basalt as mineral admixture on hydration and microstructure formation mechanism of cement, Constr. Build. Mater. 48 (2013) 434–440.
[23] M.E.S. Saraya, Study the pozzolanic activity of fresh basalt, Journal of Materials Science and Engineering. A 1 (6A) (2011) 790.
[24] H. Assaedi, T. Alomayri, F.U. Shaikh, I.M. Low, Characterisation of mechanical and thermal properties in flax fabric reinforced geopolymer composites, J. Adv. Ceram. 4 (4) (2015) 272–281.
[25] P. Amuthakkannan, V. Manikandan, J.W. Jappes, M. Uthayakumar, Effect of fibre length and fibre content on mechanical properties of short basalt fibre reinforced polymer matrix composites, Materials Physics and Mechanics 16 (2) (2013) 107–117.
[26] D. Shen, X. Liu, Q. Li, L. Sun, W. Wang, Early-age behavior and cracking resistance of high-strength concrete reinforced with Dramix 3D steel fiber, Constr. Build. Mater. 196 (2019) 307–316.
[27] P. Zhang, Y. Zheng, K. Wang, J. Zhang, A review on properties of fresh and hardened geopolymer mortar, Compos. B Eng. 152 (2018) 79–95.
[28] P. Zhang, K. Wang, J. Wang, J. Guo, Y. Ling, Macroscopic and microscopic analyses on mechanical performance of metakaolin/fly ash based geopolymer mortar, J. Cleaner Prod. 294 (2021), 126193.
[29] P. Zhang, K. Wang, J. Wang, J. Guo, S. Hu, Y. Ling, Mechanical properties and prediction of fracture parameters of geopolymer/alkali-activated mortar modified with PVA fiber and nano-SiO2, Ceram. Int. 46 (12) (2020) 20027–20037.
[30] P. Zhang, Z. Gao, J. Wang, K. Wang, Numerical modeling of rebar-matrix bond behaviors of nano-SiO2 and PVA fiber reinforced geopolymer composites, Ceram. Int. 47 (8) (2021) 11727–11737.
[31] Z.C. Girgin, M.T. Yıldırım, Usability of basalt fibres in fibre reinforced cement composites, Mater. Struct. 49 (2016) 3309–3319.
[32] V. Fiore, T. Scalici, G. Di Bella, A. Valenza, A review on basalt fibre and its composites, Compos. B Eng. 74 (2015) 74–94.
[33] A. Sadrmomtazi, B. Tahmouresi, A. Saradar, Effects of silica fume on mechanical strength and microstructure of basalt fiber reinforced cementitious composites (BFRCC), Constr. Build. Mater. 162 (2018) 321–333.
[34] Z.C. Girgin, Effect of slag, nano clay and metakaolin on mechanical performance of basalt fibre cementitious composites, Constr. Build. Mater. 192 (2018) 70–84.
[35] Z. Wang, Q. Yu, Q. Ao, Q. Du, Mechanical properties of engineered cementitious composite containing basalt fibre, Fresenius Environ. Bull. (2020) 1997.
[36] N. Zhang, J. Zhou, G.-W. Ma, Dynamic properties of strain-hardening cementitious composite reinforced with basalt and steel fibers, International Journal of Concrete Structures and Materials 14 (1) (2020) 1–14.

[37] Q. Du, C. Cai, J. Lv, J. Wu, T. Pan, J. Zhou, Experimental investigation on the mechanical properties and microstructure of basalt fiber reinforced engineered cementitious composite, Materials 13 (17) (2020) 3796.
[38] N. Ali, O. Canpolat, Y. Aygörmez, M.M. Al-Mashhadani, Evaluation of the 12–24 mm basalt fibers and boron waste on reinforced metakaolin-based geopolymer, Constr. Build. Mater. 251 (2020), 118976.
[39] S. Yildizel, Material properties of basalt-fiber-reinforced gypsum-based composites made with metakaolin and silica sand, Mech. Compos. Mater. 56 (3) (2020) 379–388.
[40] D. Ren, C. Yan, P. Duan, Z. Zhang, L. Li, Z. Yan, Durability performances of wollastonite, tremolite and basalt fiber-reinforced metakaolin geopolymer composites under sulfate and chloride attack, Constr. Build. Mater. 134 (2017) 56–66.
[41] Standard, B., Methods of testing cement—. Determination of setting times and soundness, BS EN, 2005: p. 196-3.
[42] ASTM, A., Standard test method for compressive strength of hydraulic cement mortars (using 2-in. or [50-mm] cube specimens), Annual Book of ASTM StandardsAnnual Book of ASTM Standards 4 (1) (2013) 1–9.
[43] 348–18", A.C., Standard Test Method for Flexural Strength of Hydraulic-Cement Mortars. Designation: C, 2010. 348.
[44] C597-02, A., Standard test method for pulse velocity through concrete. Annual Book of American Society of Testing and Materials, 2002: p. 04-02.
[45] B. Standard, Concrete Paving Block-Requirements and Test Methods, BS EN 1338 (2003) 2003.
[46] H. Binici, O. Aksogan, Durability of concrete made with natural granular granite, silica sand and powders of waste marble and basalt as fine aggregate, Journal of Building Engineering 19 (2018) 109–121.
[47] H. Binici, Effect of crushed ceramic and basaltic pumice as fine aggregates on concrete mortars properties, Constr. Build. Mater. 21 (6) (2007) 1191–1197.
[48] I.S. Kishore, L. Mounika, C.M. Prasad, B.H. Krishna, Experimental study on the use of basalt aggregate in concrete mixes, SSRG Int. J. Civ. Eng 2 (2015) 39–42.
[49] J. Dong, C. Li, H. Liu, L. Zhang, J. Liu, Investigating the mechanical property and reaction mechanism of geopolymers cement with red Pisha Sandstone, Constr. Build. Mater. 201 (2019) 641–650.
[50] P. Nuaklong, V. Sata, P. Chindaprasirt, Influence of recycled aggregate on fly ash geopolymer concrete properties, J. Cleaner Prod. 112 (2016) 2300–2307.
[51] K. Rahal, Mechanical properties of concrete with recycled coarse aggregate, Build. Environ. 42 (1) (2007) 407–415.
[52] F. Puertas, S. Martínez-Ramírez, S. Alonso, T.F. Vazquez, Alkali-activated fly ash/slag cements: strength behaviour and hydration products, Cem. Concr. Res. 30 (10) (2000) 1625–1632.
[53] Y. Aygörmez, O. Canpolat, M.M. Al-mashhadani, A survey on one year strength performance of reinforced geopolymer composites, Constr. Build. Mater. 264 (2020), 120267.
[54] B. Yan, P. Duan, D. Ren, Mechanical strength, surface abrasion resistance and microstructure of fly ash-metakaolin-sepiolite geopolymer composites, Ceram. Int. 43 (1) (2017) 1052–1060.
[55] R. Mohebi, K. Behfarnia, M. Shojaei, Abrasion resistance of alkali-activated slag concrete designed by Taguchi method, Constr. Build. Mater. 98 (2015) 792–798.
[56] A. Akbarnezhad, M. Huan, S. Mesgari, A. Castel, Recycling of geopolymer concrete, Constr. Build. Mater. 101 (2015) 152–158.
[57] R. Kumar, Influence of recycled coarse aggregate derived from construction and demolition waste (CDW) on abrasion resistance of pavement concrete, Constr. Build. Mater. 142 (2017) 248–255.
[58] H. Tanyildizi, Y. Yonar, Mechanical properties of geopolymer concrete containing polyvinyl alcohol fiber exposed to high temperature, Constr. Build. Mater. 126 (2016) 381–387.
[59] P. Nuaklong, P. Jongvivatsakul, T. Pothisiri, V. Sata, P. Chindaprasirt, Influence of rice husk ash on mechanical properties and fire resistance of recycled aggregate high-calcium fly ash geopolymer concrete, J. Cleaner Prod. 252 (2020), 119797.
[60] Z. Pan, J.G. Sanjayan, F. Collins, Effect of transient creep on compressive strength of geopolymer concrete for elevated temperature exposure, Cem. Concr. Res. 56 (2014) 182–189.
[61] T. Bakharev, Thermal behaviour of geopolymers prepared using class F fly ash and elevated temperature curing, Cem. Concr. Res. 36 (6) (2006) 1134–1147.
[62] Y. Aygörmez, O. Canpolat, M.M. Al-mashhadani, M. Uysal, Elevated temperature, freezing-thawing and wetting-drying effects on polypropylene fiber reinforced metakaolin based geopolymer composites, Constr. Build. Mater. 235 (2020), 117502.
[63] X. Jiang, R. Xiao, M. Zhang, W. Hu, Y. Bai, B. Huang, A laboratory investigation of steel to fly ash-based geopolymer paste bonding behavior after exposure to elevated temperatures, Constr. Build. Mater. 254 (2020), 119267.
[64] Zhang, H.Y., Kodur, V., Wu, B., Cao, L., and Qi, S.L., Comparative thermal and mechanical performance of geopolymers derived from metakaolin and fly ash. Journal of Materials in Civil Engineering, 2016. 28(2): p. 04015092.
[65] P. He, D. Jia, T. Lin, M. Wang, Y. Zhou, Effects of high-temperature heat treatment on the mechanical properties of unidirectional carbon fiber reinforced geopolymer composites, Ceram. Int. 36 (4) (2010) 1447–1453.
[66] D.L. Kong, J.G. Sanjayan, K. Sagoe-Crentsil, Comparative performance of geopolymers made with metakaolin and fly ash after exposure to elevated temperatures, Cem. Concr. Res. 37 (12) (2007) 1583–1589.
[67] J. Strzałkowski, H. Garbalińska, The Influence of Silica Fume on the Mechanical and Thermal Parameters of Portland Cement Concretes. Journal of, Ecol. Eng. 20 (9) (2019).
[68] I.B. Topçu, C. Karakurt, Properties of reinforced concrete steel rebars exposed to high temperatures. Research Letters, Mater. Sci. (2008. 2008.).
[69] R. Ghosh, S.P. Sagar, A. Kumar, S.K. Gupta, S. Kumar, Estimation of geopolymer concrete strength from ultrasonic pulse velocity (UPV) using high power pulser, Journal of building engineering 16 (2018) 39–44.
[70] Z. Yunsheng, S. Wei, L. Zongjin, Z. Xiangming, C. Chungkong, Impact properties of geopolymer based extrudates incorporated with fly ash and PVA short fiber, Constr. Build. Mater. 22 (3) (2008) 370–383.
[71] F. Puertas, T. Amat, A. Fernández-Jiménez, T. Vázquez, Mechanical and durable behaviour of alkaline cement mortars reinforced with polypropylene fibres, Cem. Concr. Res. 33 (12) (2003) 2031–2036.
[72] H. Binici, R. Gemci, A. Kucukonder, H.H. Solak, Investigating sound insulation, thermal conductivity and radioactivity of chipboards produced with cotton waste, fly ash and barite, Constr. Build. Mater. 30 (2012) 826–832.
[73] A. Dureković, V. Čalogović, K. Popović, Frost resistance of OPC-CSF mortars investigated by means of repeated cycle-and one cycle-freezing test, Cem. Concr. Res. 19 (2) (1989) 267–277.
[74] M. Jin, Z. Wang, F. Lian, P. Zhao, Freeze-thaw resistance and seawater corrosion resistance of optimized tannery sludge/metakaolin-based geopolymer, Constr. Build. Mater. 265 (2020), 120730.
[75] R. Zhao, Y. Yuan, Z. Cheng, T. Wen, J. Li, F. Li, Z.J. Ma, Freeze-thaw resistance of Class F fly ash-based geopolymer concrete, Constr. Build. Mater. 222 (2019) 474–483.